Gravity-induced anisotropies in chemical waves

Istvan. Nagypal, Gyorgy. Bazsa, and Irving R. Epstein

More About This Article

The permalink http://dx.doi.org/10.1021/ja00273a015 provides access to:

- Links to articles and content related to this article
- Copyright permission to reproduce figures and/or text from this article

to expect that the increase of electron affinity in phenyl–X, occurring on perfluorination, should be smaller for the more delocalized, higher electron affinity phenyl–X compounds. This is borne out by the data in Table IV. The increase is by far the largest for the change C_6H_6 to C_6F_6, where there is also an additional boost since six rather than five fluorine atoms are introduced. The increase on perfluorination per F atom is also given in Table V. These values are seen to decrease quite regularly with increasing electron affinity of the compounds. One exception is the dicyanoperfluorobenzene for which the effect per F atom is quite large (4.2) even though this compound has the highest electron affinity. Obviously, the comparison per fluorine atom is flawed since the position of the fluorines is not taken into account. There is evidence[6d] that F substitution of four fluorine atoms in positions 2, 3, 5, and 6 is particularly effective in increasing the electron affinity of benzene, and the change from $1,4\text{-}(CN)_2C_6H_4$ to $1,4\text{-}(CN)_2C_6F_4$ involves such a substitution.

The extra electron in the perfluoro negative ions which have strongly electron-withdrawing substituents which also conjugate with the ring, like CN, NO_2, and $COCH_3$, is almost certainly in a π^*-type orbital. The consistency in the trends observed in Tables IV and V indicates that the extra electron for all the compounds involved including $C_6F_6^-$ is in a predominantly π^*-like orbital. This is in agreement with the theoretical predictions of Shchegoleva[12] for $C_6F_6^-$.

The entropy change ΔS_4° for electron attachment to C_6F_6 was found to be 7.4 cal/deg (Table III). When 1.4 cal/deg caused by the change of multiplicity (singlet to doublet)[15] is subtracted, there remains ~ 6 cal/deg. This change could be due to loosening of the vibrational frequencies in $C_6F_6^-$ and/or to a decrease of symmetry from C_6F_6 to $C_6F_6^-$. The kinetic data, see section a in the Results and Discussion section, showed that electron transfer to C_6F_6 occurs with near 100% collision efficiency even when the reaction is near thermoneutral. This result indicates that the energy difference between the $C_6F_6^-$ obtained by a vertical transition from C_6F_6 and the ground-state geometry of the $C_6F_6^-$ is not large.[14] This is compatible with a change of soft vibrations on formation of $C_6F_6^-$ or a change of symmetry number, since these two changes need not lead to a large energy change in the vertical transition. Thus adding of the electron may only flatten the D_{6h} minimum of the energy hypersurface and lead to a lowering of the nine out-of-plane deformations. Since these have already low frequencies in C_6F_6, further softening in $C_6F_6^-$ will

be particularly effective in producing a ΔS_4° increase. Due to the high symmetry of C_6F_6, symmetry number $\sigma = 12$, a loss of symmetry in $C_6F_6^-$ resulting in $\sigma = 1$ or 2 will lead to a $\Delta S_{\text{rot,sym}}^\circ \approx 5$ cal/deg. Either of the above changes may be sufficient to lead to the observed ΔS_4° result, which itself is not very accurate.

Modern ab initio MO calculations for C_6F_6 and $C_6F_6^-$ can provide useful information on the geometry and vibrational frequency changes. We hope that the present results will encourage such theoretical work. Theoretical calculations do not perform very well for fluorine compounds particularly if polarization functions and electron correlation are not included. Therefore, abandoning the high symmetry of C_6F_6 in a geometry exploration of $C_6F_6^-$ unfortunately will be very expensive but probably worthwhile.

The present result for $EA(C_6F_6) = 0.52$ eV (12.0 kcal/mol), see Table III, is much lower than the $EA(C_6F_6) \geq 1.8$ eV obtained by Lifshitz and Tiernan[9] with the endothermic negative ion electron-transfer, tandem mass spectrometer beam method. A similar large difference is observed for perfluorotoluene, $EA(C_6F_5CF_3) = 0.94$ eV (Table III) vs. $EA(C_6F_5CF_3) \geq 1.7$ eV.[9] The consistency of the present data, Tables I–V for C_6F_6 and the substituted C_6F_5X, is very strong evidence for the reliability of the present results which makes the high values[9] almost certainly wrong. Difficulties and inconsistencies encountered in the C_6F_6 determinations were reported by Lifshitz et al.[9] Thus the thresholds obtained with I$^-$ projectiles did not agree with the thresholds obtained with S$^-$, on which the determinations were based. The I$^-$ results were rejected since the S$^-$ results were supported by an observed decrease of the transfer cross section with energy, for O$^-$. This was taken to signal an exothermic electron transfer from O$^-$ to C_6F_6 and sets the limit $EA(C_6F_6) > EA(O) = 1.47$ eV. Considering that the same publication[9] reported an electron affinity for SF_6 which was too low by some 0.4 eV,[9,14] one must conclude that the method[9] is not reliable for electron affinity determinations of perfluoro hydrocarbons and SF_6.

Gravity-Induced Anisotropies in Chemical Waves

István Nagypál,[†] György Bazsa,[†] and Irving R. Epstein*

Contribution from the Department of Chemistry, Brandeis University, Waltham, Massachusetts 02254. Received November 27, 1985

Abstract: A variety of experiments are presented to illustrate that chemical wave velocities in the iron(II)–nitric acid and in the chlorite–thiosulfate reactions are profoundly affected by the convective motion of the solutions. A qualitative model is developed to interpret the—sometimes peculiar and spectacular—phenomena caused by the simultaneous cooperative effects of chemical reaction, diffusion, heat conduction, and fluid convection.

Traveling chemical waves have been observed in many chemical reactions,[1–7] all of which exhibit two common features. They are autocatalytic and they possess bistable steady states in a stirred tank reactor. Theoretical treatments, particularly of waves in the Belousov–Zhabotinskii[8–12] (BZ) and arsenite–iodate systems,[13]

have yielded significant insights into the nature of these waves and how their velocities depend upon reactant concentrations.
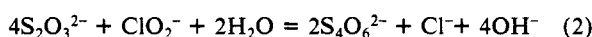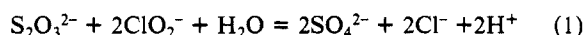
(1) Field, R. J.; Noyes, R. M. *J. Am. Chem. Soc.* **1974**, *96*, 2001.
(2) Showalter, K.; Noyes, R. M.; Turner, H. *J. Am. Chem. Soc.* **1979**, *101*, 7463.
(3) Jorne, J. *J. Am. Chem. Soc.* **1980**, *102*, 6196.
(4) Showalter, K. *J. Phys. Chem.* **1981**, *85*, 440.

†Permanent address: Department of Chemistry, Kossuth Lajos University, H-4010 Debrecen, Hungary.

3636   *J. Am. Chem. Soc., Vol. 108, No. 13, 1986*

Nagypal et al.

Bazsa and Epstein[14] have recently found that the velocity of the traveling wave in the oxidation of iron(II) by nitric acid in a tube depends crucially on the direction of travel of the wave. At some concentrations the wave moves as much as 20 times faster downward than upward. The reaction responsible for the traveling wave is exothermic; sufficient heat is generated to produce convective motion. This, however, would suggest that the wave should move faster upward, opposite to the experimental finding. This surprising result was interpreted by assuming that nucleation[15] is one of the factors which determines the wave velocity. Thus, mixing of the unreacted solution by upward convection slows down the nucleation process, while the nucleation is not affected when the wave moves downward. These experiments show that the usual consideration of chemical reaction and diffusion is not sufficient to interpret all phenomena related to chemical waves. In a gravitational field a third factor, convection, caused by the density change during the reaction may also have to be taken into account. The density of an aqueous solution during a multistep chemical reaction may change in a complex manner, influenced by the exo- or endothermicity of the reaction, by the heat exchange with the surroundings, and by the partial molar volumes of the reactants, intermediates, and products.

Chemical engineers have considered the problem of "doubly diffusive convection", in which the density of a fluid depends upon its temperature and its composition.[16] Hess and co-workers[17] have studied the coupling of glycolytic oscillations and convective patterns, while Gutkowicz-Krusin and Ross[18] and Herschkowitz-Kaufman et al.[19] have looked at the hydrodynamic stability of chemically reacting fluids in general.

We have recently studied the kinetics of the reaction between chlorite and thiosulfate at 90 °C.[20] Sulfate and chloride are the only products found, even if the thiosulfate is in excess. The reaction is catalyzed by the product hydrogen ion. Further unpublished experiments, however, show that at 25 °C two reactions take place, their ratio depending upon the initial concentration ratio of the chlorite and thiosulfate:

$$S_2O_3^{2-} + 2ClO_2^- + H_2O = 2SO_4^{2-} + 2Cl^- + 2H^+ \quad (1)$$

$$4S_2O_3^{2-} + ClO_2^- + 2H_2O = 2S_4O_6^{2-} + Cl^- + 4OH^- \quad (2)$$

The autocatalytic nature of reaction 1 thus persists at 25 °C. At pH 12 the reaction mixture remains practically unchanged for days at room temperature. If, however, a drop of acid is added at the top of an unstirred solution, the proton-catalyzed reaction speeds up, producing a frontlike chemical wave. The motion of the wave can be conveniently followed if an appropriate acid/base indicator is added to the solution. The reaction is strongly exothermic; the temperature change may be as high as 10 °C even if the reactant concentrations are only about 0.1 M. This temperature rise may result in convective motion, which—coupled with reaction and diffusion—may strongly influence the velocity of the chemical wave.

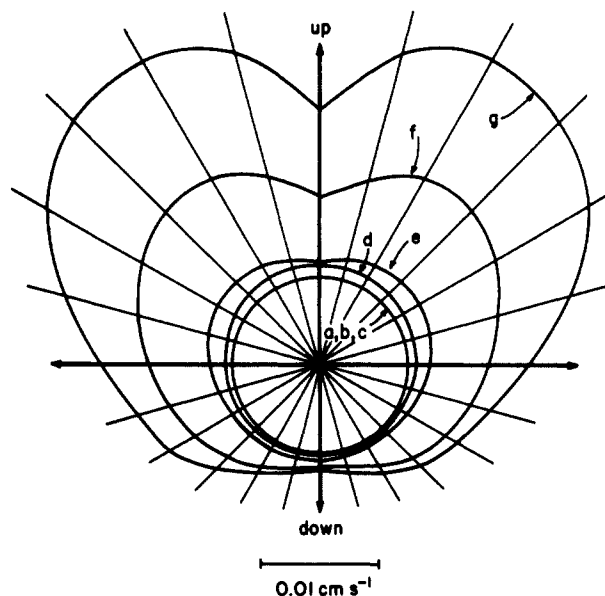The aim of our present work is to study the effect of various

up

down

0.01 cm s⁻¹

Figure 1. Velocity of the chemical wave as a function of propagation direction and internal tube diameter (i.d.) in the chlorite-thiosulfate system. $[ClO_2^-] = 0.05$ M, $[S_2O_3^{2-}] = 0.025$ M, $[OH^-] = 0.025$ M. Notations: (a–c) intramedic tubing, i.d. (mm) = 0.381 (a), 0.580 (b), 0.764 (c); (d–g) tygon tubing, i.d. (mm) = 0.794 (d), 1.584 (e), 2.381 (f), 3.175 (g).

factors, such as temperature and density changes and the heat conduction and fluid convection caused by them, on chemical wave velocities in quasi-one-dimensional tubes and to develop a unified model to interpret both earlier and our present results.

Experimental Section

Stock solutions of the reactants were freshly prepared from the highest grade chemicals commercially available. Since our earlier studies[20] had shown that recrystallization of the 85% pure sodium chlorite to better than 99% purity had no effect on the kinetics, we used the $NaClO_2$ as received from the manufacturer and established the concentration of the stock solution iodometrically. Wave-velocities in the chlorite-thiosulfate system were measured in plastic (tygon or intramedic) tubes of various diameters. The tubes were fixed vertically on a large wooden board by plastic clamps 20 cm apart and were marked with a length scale. They were filled with the solutions to be studied, and the clamps were tightly closed. Separate experiments confirmed that the waves were unable to proceed past the clamps for weeks. The waves were initiated by injection of a drop of acid at one end of the tubes and allowed to travel until the first clamp. The board was then oriented in the appropriate direction, and the waves were started by opening the first clamp. The time for each 1-cm progress of the wave was measured; the measurements were started at about 3–4 cm from the clamp and were continued to 15–16 cm, until the wave approached the next clamp. Then the whole board was repositioned to a new direction, and measurements were carried out in the next compartment.

All measurements, except for the study of the temperature dependence of the wave-velocity, were carried out at room temperature in an air-conditioned (21.5 ± 0.5 °C) laboratory. The temperature dependence of the wave-velocity was measured in a water bath at temperatures between 25 and 50 °C.

Density changes of the various solutions were determined as follows. A 300-cm³ Erlenmeyer flask was filled completely and was closed tightly with a two-hole rubber stopper. One of the holes was fitted with a temperature sensor, and the other held a long (1.5 m) scaled tygon tube of inner diameter 0.159 cm. When the stopper was inserted firmly, some solution rose in the tube. In some cases the solution in the flask was stirred vigorously with a magnetic stirrer. The temperature and the level of the solution were simultaneously measured before, during, and after the reactions. Some measurements were also carried out in a 450-cm³ Dewar flask to measure the temperature and density change under nearly adiabatic conditions.

Several experiments were performed in vertically positioned plastic Petri dishes. The solution to be studied was poured into a Petri dish cover, filling it completely. Another cover with a small (1 mm) hole drilled in the center or near the edge was gently positioned above the solution and then pressed down to provide an air-tight closure. The excess solution escaped through the hole in the upper cover. With some practice

(5) Gribschaw, T. A.; Showalter, K.; Banville, D. L.; Epstein, I. R. *J. Phys. Chem.* **1981**, *85*, 2152.

(6) Weitz, D. M.; Epstein, I. R. *J. Phys. Chem.* **1984**, *88*, 5300.

(7) Gowland, R. J.; Stedman, G. *J. Chem. Soc., Chem. Commun.* **1983**, 1038.

(8) Reusser, E. J.; Field, R. J. *J. Am. Chem. Soc.* **1979**, *101*, 1063.

(9) Schmidt, S.; Ortoleva, P. *J. Chem. Phys.* **1980**, *72*, 2733.

(10) Rinzel, J.; Ermentrout, G. B. *J. Phys. Chem.* **1982**, *86*, 2954.

(11) Shyldkrot, H.; Ross, J. *J. Chem. Phys.* **1985**, *82*, 113.

(12) Wood, P. M.; Ross, J. *J. Chem. Phys.* **1985**, *82*, 1924.

(13) Hanna, A.; Saul, A.; Showalter, K. *J. Am. Chem. Soc.* **1982**, *104*, 3838.

(14) Bazsa, G.; Epstein, I. R. *J. Phys. Chem.* **1985**, *89*, 3050.

(15) Roux, J. C.; De Kepper, P.; Boissonade, J. *J. Phys. Lett.* **1983**, *97*, 168.

(16) Turner, J. S. *Ann. Rev. Fluid Mech.* **1985**, *17*, 11.

(17) Mueller, S. C.; Plesser, T.; Hess, B. *Springer Ser. Synergetics* **1985**, *29*, 194.

(18) Gutkowicz-Krusin, D.; Ross, J. *J. Chem. Phys.* **1980**, *72*, 3577, 3588.

(19) Herschkowitz-Kaufman, M.; Nicholis, G.; Nazarea, A. *Z. Flugwiss. Weltraumforsch.* **1978**, *2*, 379.

(20) Nagypal, I.; Epstein, I. R.; Kustin, K. *Int. J. Chem. Kinet.* **1986**, *18*, 345.

(and luck), the space between the covers can be filled without any air bubbles. If the hole is small enough the closed dish can be positioned vertically without leaking. Waves were initiated either by adding a small drop of the reacted solution or by blowing an appropriate gas (NO_2 or HCl) around the hole.

Results and Discussion

The variety of experimental configurations, the surprising nature of the results, and the ongoing interaction between the model and the experiments suggest that the results are best presented in conjunction with the development of the model. Thus our exposition will be more chronological than is often the case in the presentation of less complex phenomena.

One-Dimensional Waves in the Chlorite–Thiosulfate System.

Our initial measurements, shown in a polar coordinate plot in Figure 1, were of the velocity of chemical waves traveling in various directions in a chlorite–thiosulfate solution. Measurements were made in two types of tubes (tygon and intramedic) with several different inner diameters. The average standard deviation of the measured velocities in several replicate measurements was less than 2%.

The surprising "pumpkin" shape of the velocity distributions in Figure 1 contains several features worthy of further discussion. We note here the four most significant and deal separately below with their interpretation.

(1) In the tubes with larger inner diameters, the waves move much more rapidly upward than downward. The reaction is exothermic, as is the iron(II)–nitric acid system, yet in that reaction the opposite relation was found. Thus the nucleation-based interpretation[14] offered for the velocity anisotropy in that system cannot hold in the present system. A much simpler explanation, the upward convective motion generated by the exothermic reaction, explains the chlorite–thiosulfate results satisfactorily.

(2) The maximum velocity in the thick tubes is *not* in the upward vertical direction, but is at about 40–60° from the horizontal. At 60–90°, the vertical component of the wave velocity is greater than the velocity of the upward vertical wave. We offer the following qualitative "explanation" for this observation. The horizontal (elliptical) cross section of an inclined tube is larger than the perpendicular (circular) cross section. One may view the waves, then, as traveling up a wider elliptical tube, which offers less resistance to the convective motion. On the other hand, in inclined tubes the waves travel shorter distances before reaching the wall. The interplay between these two opposing effects will yield a maximum velocity at intermediate orientations.

(3) The change from intramedic (i.d. = 0.764 mm, o.d. = 1.22 mm) to tygon (i.d. = 0.794 mm, o.d. = 2.382 mm) tubing causes a considerable anisotropy in the wave velocity (curves c and d). The small increase in the inner diameter is unlikely to be responsible for such a dramatic effect. Presumably other factors related to the wall thickness exert a significant influence on the velocity. We shall deal with this problem later.

(4) Curves a, b, and c show that the effect of convective motion can be successfully eliminated; the velocity in these thin tubes is independent of direction and of the tube diameter. Thus, if the concentration dependence of the velocity is to be studied and modeled by reaction-diffusion equations, then the experiments must be conducted in convection-free thin tubes or layers.

We have measured the concentration dependence of the isotropic wave velocities using intramedic (i.d. = 0.764 mm, o.d. = 1.22 mm) tubes. The initial concentrations of the solutions studied are summarized in Table I, which also contains the measured velocity and the calculated hydrogen ion concentration $[H^+]_b$ of the solution behind the wave. According to eq 1 and 2, if $[ClO_2^-]/[S_2O_3^{2-}] > 2$, then $[H^+]_b = 2[S_2O_3^{2-}] - [OH^-]$. If, however, $1/4 < [ClO_2^-]/[S_2O_3^{2-}] < 2$ then $[H^+]_b = (12/7)[ClO_2^-] - (10/7)[S_2O_3^{2-}] - [OH^-]$. No wave occurs if the calculated $[H^+]_b$ is negative.

The last column of Table I shows the experimentally determined hydrogen ion concentration measured in separate well-mixed samples. It is seen from the table that the measured $[H^+]_b$ agrees with the calculated one only if $[ClO_2^-]/[S_2O_3^{2-}] > 2$, i.e., when the first reaction takes place exclusively (numbers 14–17). When

Table I. Concentration Dependence of the Isotropic Wave Velocity

no.	$[ClO_2^-]$, M	$[S_2O_3^{2-}]$, M	$[OH^-]$, M	v, mm/min	$[H^+]_{b,calcd}$, M	$[H^+]_{b,exptl}$, M
1	0.0497	0.0250	0.0078	14.67	0.0417	0.0335
2	0.0497	0.0250	0.0128	11.28	0.0367	0.0283
3	0.0497	0.0250	0.0178	8.37	0.0316	0.0239
4	0.0497	0.0250	0.0228	5.84	0.0269	0.0194
5	0.0497	0.0250	0.0278	3.55	0.0217	0.0150
6	0.0497	0.0250	0.0128	11.44	0.0367	0.0282
7	0.0447	0.0250	0.0126	8.60	0.0283	0.0223
8	0.0397	0.0250	0.0124	5.50	0.0199	0.0159
9	0.0348	0.0250	0.0122	2.28	0.0117	0.0091
10	0.0497	0.0375	0.0132	4.03	0.0184	0.0152
11	0.0497	0.0312	0.0130	8.30	0.0276	0.0221
12	0.0497	0.0287	0.0129	9.74	0.0313	0.0250
13	0.0497	0.0250	0.0128	11.34	0.0367	0.0289
14	0.0497	0.0212	0.0127	12.43	0.0297	0.0300
15	0.0497	0.0187	0.0126	10.64	0.0248	0.0247
16	0.0497	0.0162	0.0125	7.78	0.0199	0.0200
17	0.0497	0.0125	0.0124	2.49	0.0126	0.0124
18	0.0347	0.0175	0.0200	2.07	0.0145	0.0100
19	0.0397	0.0200	0.0200	3.59	0.0195	0.0140
20	0.0447	0.0225	0.0200	5.24	0.0245	0.0180
21	0.0497	0.0250	0.0200	6.64	0.0295	0.0220
22	0.0546	0.0275	0.0200	8.43	0.0343	0.0261
23	0.0596	0.0300	0.0200	10.01	0.0393	0.0302
24	0.0671	0.0338	0.0200	12.59	0.0467	0.0366
25	0.0745	0.0375	0.0200	15.18	0.0541	0.0438
26	0.0820	0.0412	0.0200	17.57	0.0617	0.0499
27	0.0894	0.0450	0.0200	20.72	0.0690	0.0567
28	0.0994	0.0500	0.0200	24.35	0.0790	0.0660

the thiosulfate concentration exceeds this ratio, then considerably less hydrogen ion is produced than calculated. In these solutions, however, no unreacted chlorite or thiosulfate may remain, because the chlorite would oxidize the tetrathionate and the thiosulfate would decompose at this acidity. Thus, the deviation must result from the occurrence of side reactions which produce other polythionates and/or chlorate.

Table I shows that the main factor determining the velocity of the wave is $[H^+]_b$.[21] A detailed numerical analysis reveals that the initial OH^- concentration also influences the wave velocity. The velocities can be described to good accuracy by the empirical equation

$$v = a[H^+]_b + b[OH^-] \qquad (3)$$

with $a = 0.74$ cm s^{-1} M^{-1} and $b = -0.22$ cm s^{-1} M^{-1}. A fit of the experimental points to a straight line, given by dividing both sides of eq 3 by $[OH^-]$, is shown in Figure 2.

In principle, the concentration dependence of the wave velocity may be calculated by analytical or numerical solution of the reaction-diffusion equations for the system. In the present case, however, the rate equation for the autocatalytic part of the reaction (at 25 °C) is still unknown, thus a theoretical treatment of the concentration dependence of the wave velocity must be postponed until the mechanism of the reaction is established.

The Ferrous–Nitric Acid System: Density–Time Profiles.

In order to shed light on the apparent contradiction between the velocity anisotropies found earlier in the iron(II)–nitric acid system and those in the present chlorite–thiosulfate system, we measured the volume and temperature changes during the course of the reaction as described in the Experimental Section. Figure 3 shows the temperature and volume changes as functions of time in a solution initially containing 0.2 M Fe^{2+} and 3 M HNO_3. The starting solution is somewhat warmer than the environment, because of the heat liberated when the reactants are mixed; thus the solution first cools down. After about 15 min the autocatalytic reaction speeds up, and the temperature and the volume increase. The reaction is over in a few minutes, and the product solution starts to cool again. The temperature–time profile is roughly the same in both cooling stages, but the volume decreases much more sharply in the second, post-reaction cooling. Renormalizing the
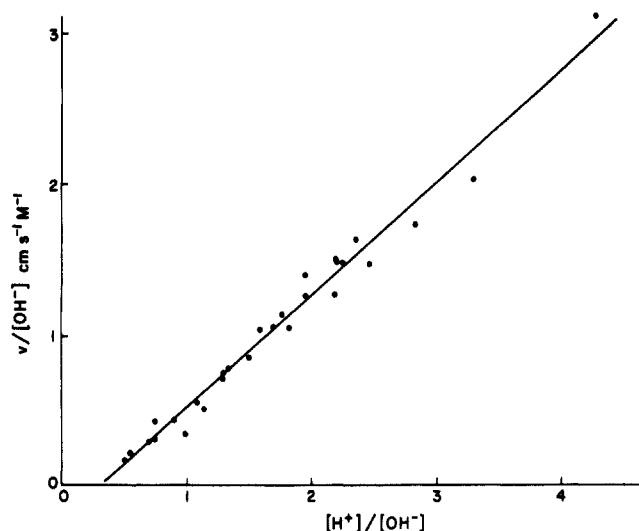
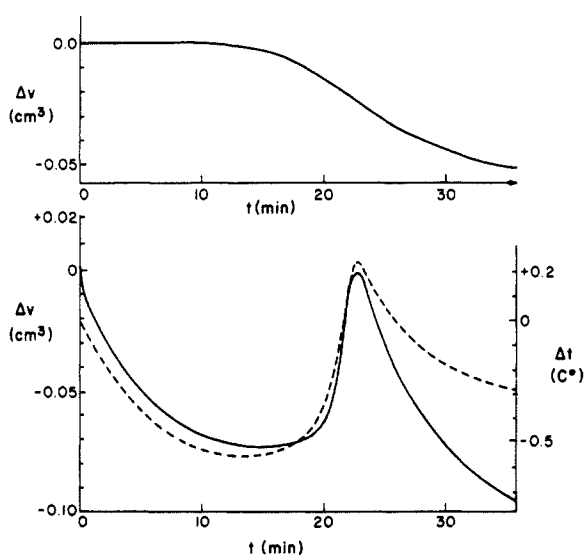**Figure 2.** Linearized form of eq 3 (see text).

Figure 3. Lower curves: temperature (dashed line) and volume (full line) changes in a 300-cm^3 solution containing 0.2 M Fe^{2+} and 3 M HNO$_3$ during the course of the reaction. Upper curve: volume change in the same solution calculated by assuming a hypothetical isothermal reaction (see text).

Figure 4. Schematic illustration of the processes taking place in the Fe^{2+}-nitric acid system. Notations: a high concentration of dots indicates the reacted sphere, a lesser concentration of dots indicates unreacted solution surrounding the reacted sphere, slants indicate the bulk unreacted solution, and wavy arrows indicate heat dissipation. T = temperature; S = density. For further explanation, see text.

volume to the initial temperature, we find that if the reaction were isothermal, then it would be accompanied by a significant increase in density. This isothermal volume change is plotted in the upper half of Figure 3. The curve was calculated from the experimental volume–time curve using the independently determined thermal expansion coefficients, which were found to be essentially the same before and after the reaction.

A Model. In light of this experiment we propose a model to explain the behavior found in the iron(II)–nitric acid system. For simplicity, several nearly simultaneous processes are illustrated stepwise in Figure 4. In what follows we assume that the density of the fluid varies independently with its temperature and composition. Under the conditions of our experiments, this approximation should be quite accurate.

Suppose that the reaction is initiated in a small sphere. The temperature rises within this sphere because of the heat of reaction. The temperature in a larger sphere surrounding the reacted sphere at this moment is equal to that of the bulk solution, and the density of the reacted sphere is less than the density of the environment (Figure 4a). Heat exchange takes place between the reacted sphere and its unreacted environment, leading to the relations illustrated in Figure 4b. As the isothermal density of the reacted sphere is greater than that of the unreacted environment, the density of the reacted sphere exceeds that of the environment
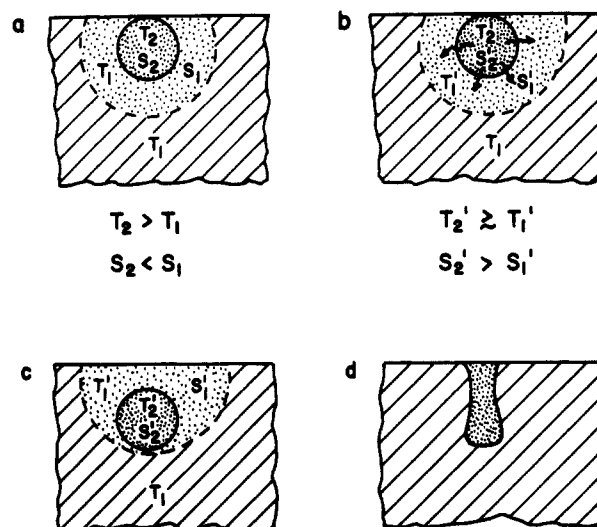
before the complete heat exchange takes place. Thus the warmer but heavier reacted sphere "drops" down (Figure 4c). These processes—together with diffusion and chemical reaction—occur simultaneously, without a sharp break. The observable net effect is a downward extension of the reacted sphere, as illustrated in Figure 4d.

The key point is that two opposing effects are present simultaneously. The heat of reaction tends to cause upward convection, while the isothermal density increase leads to downward convection. If the reaction is rapid, and/or the heat of reaction is high, then the heat dissipation cannot compensate for the density decrease caused by the rising temperature. The net result is then an upward convection. If, however, the reaction is relatively slow, or the reaction heat is small, then there is sufficient time for heat dissipation into the unreacted environment and thus a downward convection takes place. This latter situation occurs in the iron-(II)–nitric acid system,[14] where the adiabatic temperature change (measured in a Dewar flask, instead of an Erlenmeyer) is only 1.75 °C, even if the initial concentrations are 0.2 M Fe^{2+} and 3 M HNO$_3$.

In agreement with the above considerations, Fe^{2+}–HNO$_3$ waves initiated in vertical Petri dishes form "streamers", which move downward with stunningly high velocity (5–15 cm/min). Waves initiated in the middle of a vertical Petri dish in the chlorite–thiosulfate system with concentrations of about 0.06 M ClO$_2^-$, 0.03 M S$_2$O$_3^{2-}$, and 0.01 M OH$^-$ first "climb" quickly in a narrow trail. Then the reaction starts at the top of the dish and a smooth horizontal reaction front moves down.

One might infer from the above observations that the isothermal density in the chlorite–thiosulfate reaction decreases. Simultaneous volume and temperature measurements, however, show that the isothermal density actually increases in this system, too, by about 0.0002 g/cm^3. Thus, if our model is correct, then an appropriate decrease in the concentrations should produce a chlorite–thiosulfate wave that travels more rapidly in the downward direction. Further experiments confirm this prediction. A tenfold decrease of the initial concentrations (0.006 M ClO$_2^-$, 0.003 M S$_2$O$_3^{2-}$, 0.001 M OH$^-$) causes the wave to start downward in the vertical Petri dish. We have also repeated the direction and diameter-dependence studies at much lower concentrations. The results are illustrated in Figure 5. In thick tubes we obtain almost the mirror image of the "pumpkin-shaped" velocity distribution found at higher concentration in Figure 1.

Further Observations. The effect of varying the total concentration is shown in Figure 6, where the ratio of the reactant concentrations is maintained constant, but the total concentration
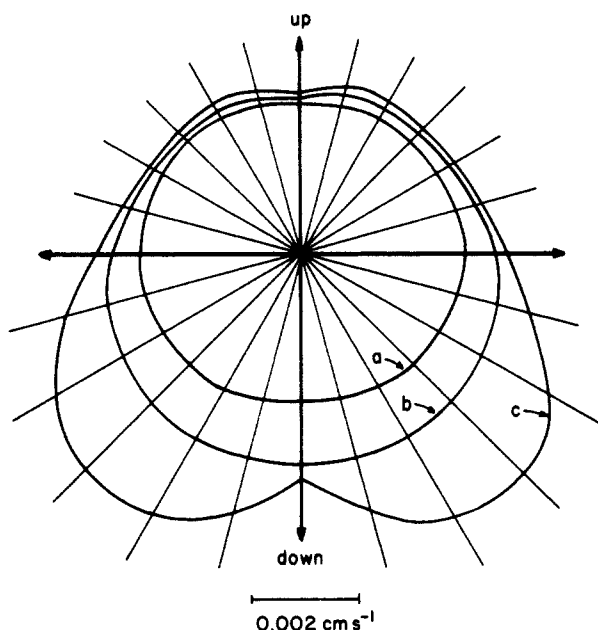
Figure 5. Velocity of the chemical wave in the chlorite–thiosulfate system as a function of direction and tube diameter. $[ClO_2^-]$ = 0.009 M, $[S_2O_3^{2-}]$ = 0.0045 M, $[OH^-]$ = 0.002 M. i.d. (mm) = 0.794 (a), 3.17 (b), 4.76 (c), tygon tubing.

Table II. Upward and Downward Velocities (cm s^{-1}) of Chemical Waves in the Chlorite–Thiosulfate Reaction in a Tube Immersed in Air or Water[a]

	upward	downward
in air	0.0165	0.0141
in water	0.0121	0.0141

[a] Tygon tubing, i.d. 3.17 mm, $[ClO_2^-]$ = 0.0275 M, $[S_2O_3^-]$ = 0.0137 M, $[OH^-]$ = 0.0055 M.

is varied. At low concentrations the downward velocity is greater and is nearly proportional to the concentration. The upward velocity, however, increases sharply at about $[ClO_2^-]$ = 0.025 M, where the heat production overtakes the effect of heat dissipation.

The importance of heat conduction was further confirmed by measuring the velocity of the wave in a tube immersed first in air and then in water at the same temperatue. The results are summarized in Table II. The downward velocity is independent of the medium surrounding the tube, but the upward velocity depends strongly upon the medium. The more effective water cooling slows the upward wave relative to the upward wave in the air-cooled tube to the extent that the relation between the upward and downward velocities is reversed. These findings suggest that the difference between the intramedic and tygon tubings results from the fact that heat transfer through a thin plastic wall is more effective than heat transfer through a thick wall.

To investigate further the assumption that reaction and diffusion are the only factors that determine the wave velocities in thin tubes, we measured the temperature dependence of the horizontal wave velocities in tubes of several different diameters. The results are shown in Figure 7. The Arrhenius plot for the thin tubes gives a straight line, as would be expected for any multiplicative combination of the reaction and diffusion rates. For the thicker tubes, however, the points show significant curvature, suggesting the influence of additional factors.

The reactions were also studied in horizontal Petri dishes which allowed for propagation of essentially two-dimensional waves. It was found earlier[14] that in a 3 M HNO_3 and 0.2 M Fe^{2+} solution the depth of the solution layer had a profound effect on the waves. The times from initiation of the waves to arrival at the wall were about 30, 20, 5, and 3 min at depths of 1, 2, 3, and 4 mm, respectively; i.e., the waves were much faster in the thicker layer. The same ordering was found in the chlorite–thiosulfate system at relatively high concentrations (0.06 M ClO_2^-, 0.03 M $S_2O_3^{2-}$, and 0.03 M OH^-). With a tenfold dilution of the chlorite–thio-
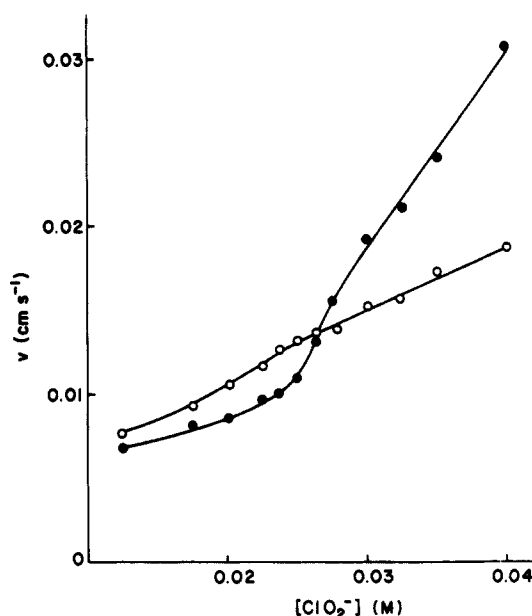

Figure 6. Upward (●) and downward (O) velocities of chemical waves in the chlorite–thiosulfate system in i.d. = 3.17 mm tygon tubing as a function of the chlorite concentration at constant concentration ratios of the reactants ($[ClO_2^-]/[S_2O_3^{2-}]$ = 2.00; $[ClO_2^-]/[OH^-]$ = 4.50).
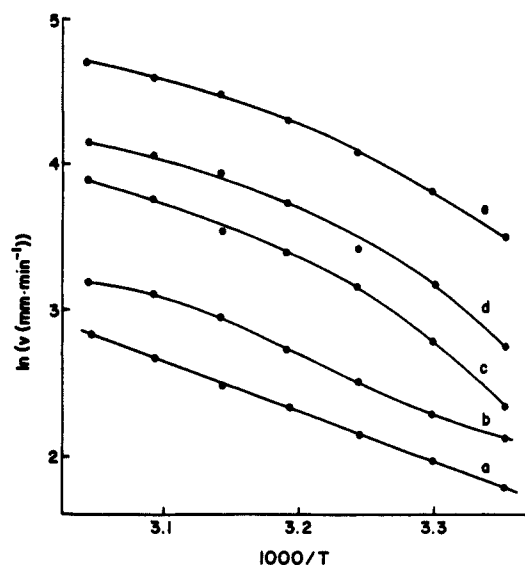

Figure 7. Wave velocities in the chlorite–thiosulfate system ($[ClO_2]$ = 0.05 M, $[S_2O_3^{2-}]$ = 0.025 M, $[OH^-]$ = 0.015 M) as a function of temperature in horizontal tubes of different diameters: (a) coincident points measured in intramedic, i.d. = 0.583 mm and tygon, i.d. = 0.794 mm tubes; (b) i.d. = 1.59 mm; (c) i.d. = 2.38 mm; (d) i.d. = 3.17 mm; (e) i.d. = 4.76 mm. (b–e curves were measured in tygon.)

sulfate solution, the *reverse order* was found; i.e., the wave moves faster in the thin layer than in the thick one. Careful visual observation of the waves shows that—at least in the 3- and 4-mm layers—the circular wave at the surface at high concentration is considerably (3–5 mm) wider than at the bottom, while the opposite relation holds at low concentration. Clearly, reaction-diffusion equations are insufficient to model such waves.

The interplay of opposing effects leads to a rather spectacular phenomenon in a relatively thick (i.d. = 4.76 mm) horizontal tube at 0.009 M ClO_2^-, 0.0045 M $S_2O_3^{2-}$, and 0.002 M OH^- concentrations. If a wave is initiated at the bottom of the tube, then the reaction front assumes a smooth shape, illustrated in Figure 8a, and the front moves steadily and smoothly without changing its shape. If, however, the wave is initiated at the top, then the drop starts to fall quickly. This induces a chemical reaction around the drop, which leads to an intense heat production. Thus, after a few seconds, an opposite upward convection is initiated. The
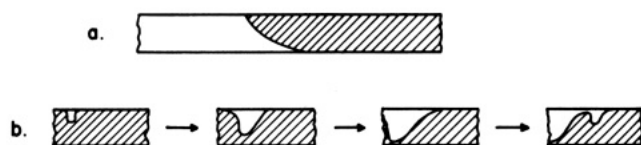
Figure 8. Schematic illustration of (a) the stable smooth and (b) the unstable "rolling" wave in a horizontal thick (i.d., = 4.76 mm) tube. ($[ClO_2^-]$ = 0.009 M, $[S_2O_3^{2-}]$ = 0.0045 M, $[OH^-]$ = 0.002 M.)
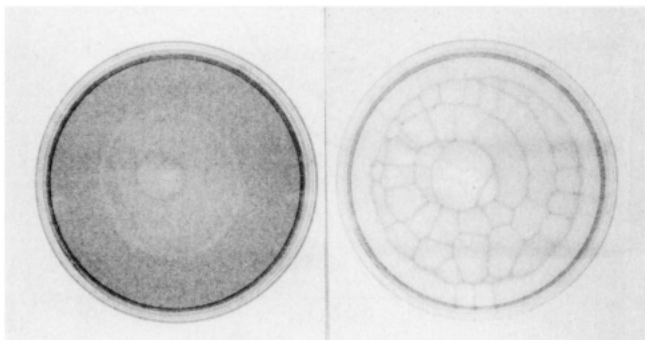

Figure 9. Concentric rings and mosaic patterns in a horizontal Petri dish (see text).

shape of the resulting front is the mirror image of the stable front. This front is unstable, and when the upper reacted portion cools, a new drop is formed, starting from the top of the tube again, as illustrated in Figure 8b. Thus one observes a "rolling" chemical wave, whose overall velocity is about 3–4 times higher than that of the stable front (Figure 8a). The "rolling" wave leaves behind unreacted zones, which slowly disappear. Exactly the same process takes place if the wave is initiated in the quasi-two-dimensional horizontal Petri dish, with the same thickness and reagent concentrations. In this case, however, concentric rings remain unreacted behind the front. The production of concentric rings in a reaction mixture which is neither oscillatory nor excitable is a striking demonstration of the importance of considering convective effects when investigating traveling waves. The slowly disappearing rings can also leave a mosaic pattern reminiscent of those reported by Avnir et al.[22] Both the concentric ring and mosaic patterns are illustrated in Figure 9.

Finally, temperature and density measurements in the arsenite–iodate system show that the reaction is exothermic and is accompanied by a *decrease* in the isothermal density. In this system, therefore, both effects act in the same direction. Thus the upward velocity should exceed the downward velocity for all concentrations.

Conclusion

The results presented in this paper argue strongly that previous chemical wave studies should be reanalyzed to assess the possible results of reaction exothermicity, convection, and heat conduction. This fact should be kept in mind by those studying chemical instabilities in unstirred spectrophotometer cells. As several groups[23-25] have shown in the case of photochemical oscillators, it is remarkably difficult to eliminate convection.

Perhaps the most surprising result in the present investigation is the magnitude of the isothermal density changes which takes place in the reactions studied. By taking account of this phenomenon we have been able to construct a model which reconciled the apparently contradictory results in the Fe^{2+}–HNO_3 and ClO_2^-–$S_2O_3^{2-}$ experiments and even allowed us to "invert the pumpkin" in the chlorite–thiosulfate velocity distributions. The "rolling waves" and concentric rings provide further support for the model.

More quantitative treatments of the phenomena discussed here are clearly called for, but they are likely to be extremely complex. Designing experiments to avoid or at least to minimize gravitational effects may be a more attractive option. While one might consider experiments in gravitation-free orbit, the use of sufficiently thin tubes would seem to provide a more accessible and less expensive solution to this problem.

(21) Note that although the initial concentrations of ClO_2^- and $S_2O_3^{2-}$ do not appear explicitly in eq 3, they influence the wave velocity via their effect on $[H^+]_b$.

(22) Avnir, D.; Kagan, M. *Nature (London)* **1984**, *307*, 717.

(23) Laplante, J. P.; Pottier, R. H. *J. Phys. Chem.* **1982**, *86*, 4759.

(24) Epstein, I. R.; Morgan, M.; Steel, C.; Valdes-Aguilera, O. *J. Phys. Chem.* **1983**, *87*, 3955.

(25) Pearlstein, A. J. *J. Phys. Chem.* **1985**, *89*, 1054.

Valence and Molecular Structure

Karl Jug,* Nicolaos D. Epiotis,[†] and Sabine Buss

Contribution from the Theoretische Chemie, Universität Hannover, 3000 Hannover 1, Federal Republic of Germany. Received November 5, 1985

Abstract: The relation between bond valence and stability of molecules is further investigated. Different geometrical arrangements of molecules are compared with respect to valence, charge, occupation numbers, and total energy. It is demonstrated that the ionicity of molecules can be described by the bond number resulting from atomic valence numbers. It is also shown that ideas of bonding expressed in the recent molecular orbital valence bond (MOVB) theory can be quantified with valence.

1. Introduction

Many years ago, Pauling[1] advocated an explanation of the structure of molecules by valence bond theory. In this theory it is natural to attach special meaning to each of the bonds and

consider the whole molecule in terms of its bond properties. One of the questions that arises is the problem of the partial ionic character of covalent bonds. The amount of ionic character is determined by the importance of the ionic structure in the total

†Alexander von Humboldt Awardee. Permanent address: Department of Chemistry, University of Washington, Seattle, WA 98195.

(1) Pauling, L. *The Nature of the Chemical Bond*, 3rd ed.; Cornell University: Ithaca, NY, 1960; p 64 ff.